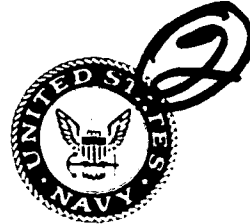


DTIC FILE COPY

Naval Research Laboratory

Washington, DC 20375-5000



NRL Memorandum Report 6726

AD-A227 547

Ohmic Effects in Quasioptical Resonators

T. A. HARGREAVES, R. P. FISCHER AND R. B. MCCOWAN

*Beam Physics Branch
Plasma Physics Division*

October 9, 1990

DTIC
ELECTE
OCT 12 1990
S E D
Ca

REPORT DOCUMENTATION PAGE			Form Approved OMB No. 0704-0188	
Public reporting burden for this collection of information is estimated to average 1 hour per response, including the time for reviewing instructions, searching existing data sources, gathering and maintaining the data needed, and completing and reviewing the collection of information. Send comments regarding this burden estimate or any other aspect of this collection of information, including suggestions for reducing this burden, to Washington Headquarters Services, Directorate for Information Operations and Reports, 1215 Jefferson Davis Highway, Suite 1204, Arlington, VA 22202-4302, and to the Office of Management and Budget, Paperwork Reduction Project (0704-0188), Washington, DC 20503				
1. AGENCY USE ONLY (Leave blank)	2. REPORT DATE 1990 October 9	3. REPORT TYPE AND DATES COVERED Interim		
4. TITLE AND SUBTITLE Ohmic Effects in Quasioptical Resonators		5. FUNDING NUMBERS JO #47-3020-A-0		
6. AUTHOR(S) T. A. Hargreaves, R. P. Fischer, and R. B. McCowan				
7. PERFORMING ORGANIZATION NAME(S) AND ADDRESS(ES) Naval Research Laboratory Washington, DC 20375-5000		8. PERFORMING ORGANIZATION REPORT NUMBER NRL Memorandum Report 6726		
9. SPONSORING / MONITORING AGENCY NAME(S) AND ADDRESS(ES) U. S. Department of Energy Washington, DC 20545		10. SPONSORING / MONITORING AGENCY REPORT NUMBER		
11. SUPPLEMENTARY NOTES				
12a. DISTRIBUTION / AVAILABILITY STATEMENT Approved for public release; distribution unlimited.		12b. DISTRIBUTION CODE		
13. ABSTRACT (Maximum 200 words) Several properties of the Fabry-Perot-type open resonator used in the quasioptical gyrotron (QOG) and the quasioptical induced resonance electron cyclotron (IREC) maser are derived. The electric fields of the normal modes are given for the general case of the resonator axis tilted with respect to the direction perpendicular to the electron beam axis. The ohmic quality factor and the power dissipated in the mirrors is derived, as is the energy stored in the resonator. The time dependence of the mirror heating, useful for pulsed experiments, is also derived. The formulae are applied to an example of current relevance, the IREC maser resonator.				
14. SUBJECT TERMS Quasioptical Quasioptical resonators		Ohmic heating		15. NUMBER OF PAGES 29
				16. PRICE CODE
17. SECURITY CLASSIFICATION OF REPORT UNCLASSIFIED	18. SECURITY CLASSIFICATION OF THIS PAGE UNCLASSIFIED	19. SECURITY CLASSIFICATION OF ABSTRACT UNCLASSIFIED	20. LIMITATION OF ABSTRACT SAR	

CONTENTS

I.	INTRODUCTION	1
II.	CAVITY FIELDS	1
III.	OHMIC POWER LOSSES	4
IV.	STORED ENERGY	9
V.	OHMIC Q	9
VI.	RESONATOR HEATING	9
VII.	THE IREC MASER RESONATOR	11
VIII.	ACKNOWLEDGEMENTS	12
	REFERENCES	14
	DISTRIBUTION LIST	17

Accession For	
NTIS GRA&I	<input checked="" type="checkbox"/>
DTIC TAB	<input type="checkbox"/>
Unannounced	<input type="checkbox"/>
Justification	
By _____	
Distribution/	
Availability Codes	
Dist	Avail and/or Special
A-1	

OHMIC EFFECTS IN QUASIOPTICAL RESONATORS

I. Introduction

The quasioptical gyrotron (QOG) has been under investigation at NRL for several years as a potential source of high-power radiation at frequencies above 100 GHz for electron cyclotron resonance heating (ECRH) of fusion plasmas.^{1, 2, 3, 4} An integral part of the QOG is the resonator, which traps some of the radiation emitted by the electron beam, allowing the radio frequency (rf) fields to grow to the large values necessary for efficient extraction of energy from the beam. The QOG resonator suffers losses due to diffraction of the radiation around the outer edge of the resonator mirrors as well as the finite conductivity of the mirror surfaces. Clearly, it is imperative to understand each of these loss mechanisms in order to understand the operation of the QOG experiments. This note addresses the ohmic losses in the resonator, deriving expressions for the electric field in the resonator, the ohmic quality factor (Q_Ω), the ohmic heating density (ρ_Ω), the total ohmic power (P_Ω) dissipated in the resonator mirrors, and the temperature rise of the mirrors. The derived formulae are then applied to the current design of the cavity to be utilized in the NRL induced resonance electron cyclotron (IREC) maser experiment.

II. Cavity Fields

The resonator considered here consists of the Fabry-Perot-type open resonator shown in Fig. 1. The spherical cavity mirrors form an azimuthally symmetric resonator about the cavity (y') axis, which is offset by an angle θ from the y -axis as shown in Fig. 2. The angle θ is used in the QOG literature,⁵ however, in the IREC maser literature⁶ the angle ψ between the resonator (y') and the electron beam (z) axes is typically used. The mode structure and stability of this type of resonator is discussed by Yariv⁷ who finds that the electric field of the transverse electric and magnetic ($TEM_{m,n,l}$) modes of the travelling

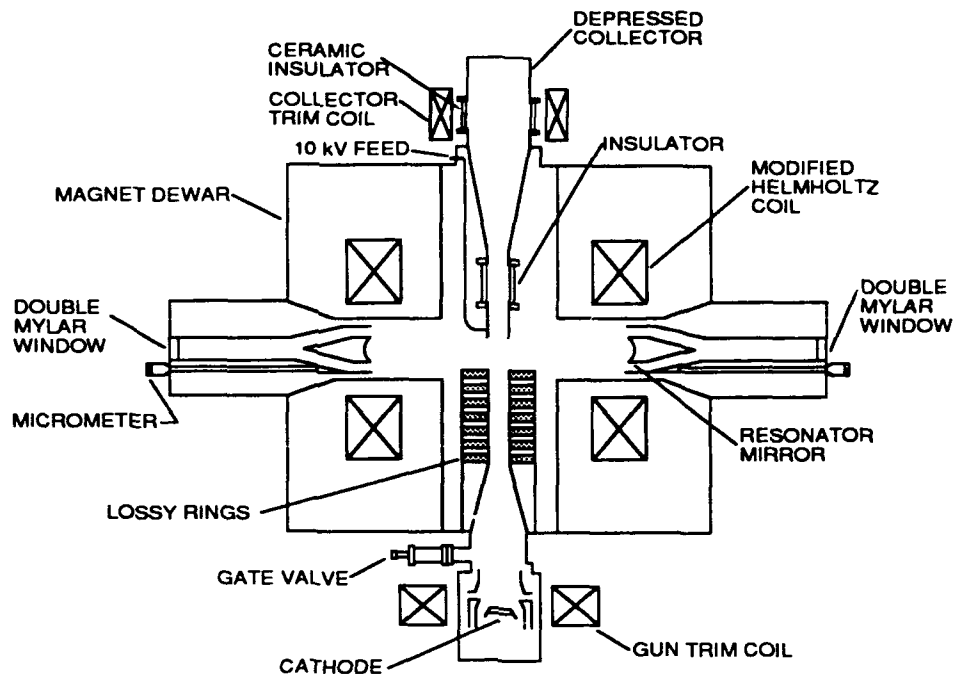


Figure 1: Schematic diagram of the quasioptical gyrotron experiment.

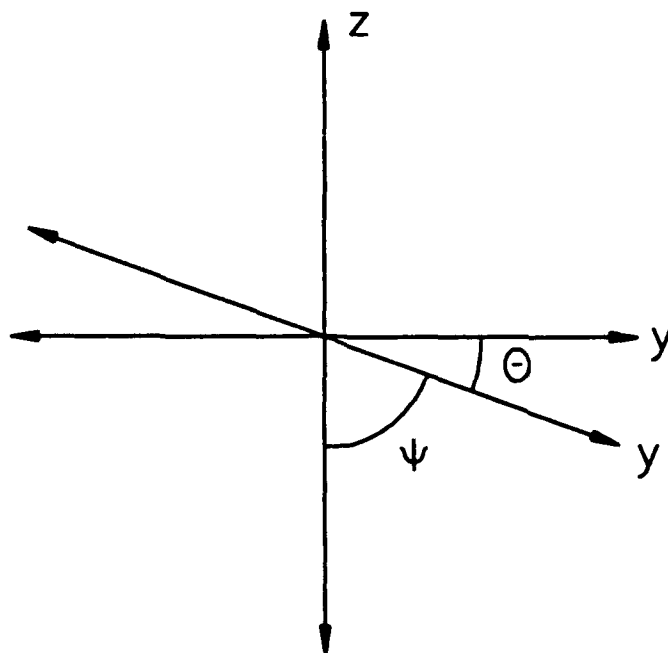


Figure 2: Orientation of the resonator (y')-axis with respect to the electron beam (z)-axis.

wave in the cavity may be expressed as

$$\mathbf{E} = \hat{x} E^t \quad (1)$$

where the physical electric field is obtained by taking the real part of \mathbf{E} , and

$$\begin{aligned} E_{m,n,l}^t(x, y', z', t) = & \frac{E_{o,l}}{2} \frac{w_{o,l}}{w_l(y')} H_m \left(\frac{\sqrt{2}x}{w_l(y')} \right) H_n \left(\frac{\sqrt{2}z'}{w_l(y')} \right) \exp \left\{ -\frac{(x^2 + z'^2)}{w_l^2(y')} \right\} \\ & \times \exp \left\{ -i \left[k_l \left(y' + \frac{(x^2 + z'^2)}{2R_w(y')} \right) - \omega_l t \right. \right. \\ & \left. \left. - (m + n + 1) \arctan \left(\frac{y'}{z_o} \right) \right] \right\} \end{aligned} \quad (2)$$

where H_m is a Hermite polynomial of order m , w_o is the radiation beam waist,

$$w_l^2(y) = w_{o,l}^2 \left(1 + y^2/z_o^2 \right), \quad (3)$$

$$R_w(y) = y \left(1 + z_o^2/y^2 \right), \quad (4)$$

$$z_o = \frac{\pi w_{o,l}^2}{\lambda} = \frac{d}{2} \left(\frac{1+g}{1-g} \right)^{1/2}, \quad (5)$$

R_w is the radius of curvature of the radiation wavefront, k is the wave number, λ is the wavelength and ω is the angular frequency of the radiation, d is the resonator mirror separation and $g = 1 - d/R_c$, where R_c is the mirror radius of curvature, which is assumed equal to the curvature of the radiation wavefront at the mirror. The electric field of the standing wave in the resonator is obtained by adding the two oppositely directed travelling waves, yielding

$$\begin{aligned} E_{m,n,l}^s(x, y', z', t) = & E_{o,l} \frac{w_{o,l}}{w_l(y')} H_m \left(\frac{\sqrt{2}x}{w_l(y')} \right) H_n \left(\frac{\sqrt{2}z'}{w_l(y')} \right) \exp \left\{ -\frac{(x^2 + z'^2)}{w_l^2(y')} \right\} \\ & \times \exp \left\{ i \left[\omega_l t + (m + n + 1) \arctan \left(\frac{y'}{z_o} \right) \right] \right\} \\ & \times \cos \left[k_l \left(y' + \frac{(x^2 + z'^2)}{2R_w(y')} \right) - \frac{l\pi}{2} \right], \end{aligned} \quad (6)$$

where the $l\pi/2$ term in the cosine is necessary to satisfy the boundary conditions at the resonator mirrors.

Of particular interest is the electric field at the electron beam, which is located very near the RF beam waist (i.e. $y' \ll z_o$). In this case $R_w \approx 0$, $w_l(y') \approx w_o$, and $\arctan(y'/z_o) \approx 0$ yielding

$$E_{m,n,l}^s(x, y', z', t) = E_{o,l} H_m \left(\frac{\sqrt{2}x}{w_{o,l}} \right) H_n \left(\frac{\sqrt{2}z'}{w_{o,l}} \right) \exp \left\{ -\frac{(x^2 + z'^2)}{w_{o,l}^2} \right\} \times \exp \{ i\omega_l t \} \cos \left(k_l y' - \frac{l\pi}{2} \right). \quad (7)$$

For the TEM_{0,0,l} mode this becomes

$$E_{0,0,l}^s(x, y', z', t) = E_{o,l} \exp \left\{ -\frac{(x^2 + z'^2)}{w_{o,l}^2} \right\} \exp \{ i\omega_l t \} \cos \left(k_l y' - \frac{l\pi}{2} \right). \quad (8)$$

The peak electric field of the TEM_{0,0,l} mode along the resonator (y' -) axis is (in MKS units)

$$E_{\text{peak}} = E_{o,l} \frac{w_{o,l}}{w_l(y')} = \frac{m_o c \omega \gamma}{e \beta_{\perp}^{s-4}} \frac{w_{o,l}}{w_l(y')} \left(\frac{\sin^2(\psi)}{(1 - \beta_{\parallel} \cos(\psi))^2} \right) \left(\frac{2^{s-1} s!}{s^s} \right) F \quad (9)$$

where F is the peak normalized wave amplitude commonly used in the gyrotron literature,^{8,9} m_o and e are the rest mass and charge (magnitude) of an electron, γ is the relativistic factor, and β_{\perp} and β_{\parallel} are the electrons velocity perpendicular and parallel to the magnetic field normalized to c , the speed of light. The parameter s is the harmonic number of the beam-wave interaction for the case of the QOG and should be set to unity for the IREC maser resonator. The angle ψ is the angle between the resonator and electron beam axes, and should be set to $\pi/2$ for the QOG.

III. Ohmic Power Losses

To calculate the ohmic power lost in the resonator mirrors, consider a plane wave incident on a semi-infinite planar conductor as shown in Fig. 3. Assuming that all field quantities \mathcal{S} vary in time as

$$\mathcal{S}(\mathbf{x}, t) = \mathbf{S}(\mathbf{x}) e^{i\omega t} \quad (10)$$

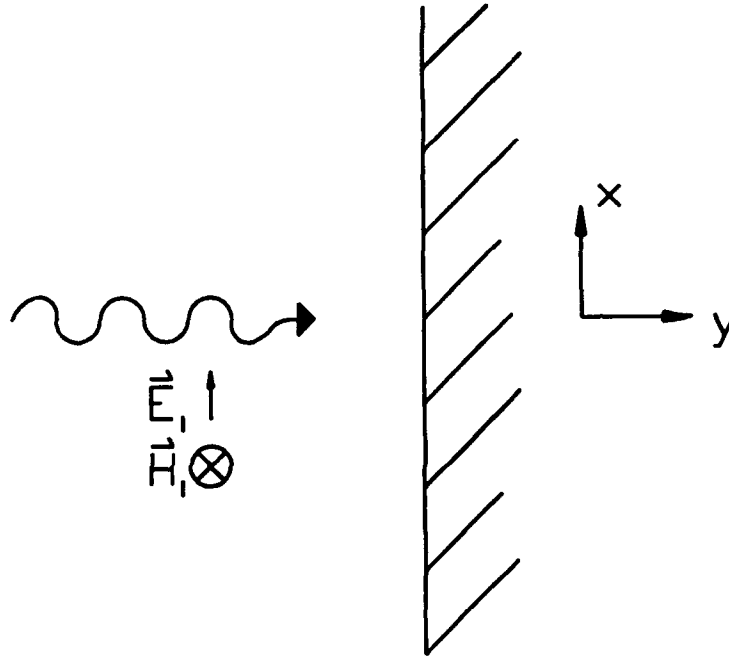


Figure 3: A plane wave incident on a semi-infinite planar conductor.

and

$$\mathbf{B} = \mu \mathbf{H} \quad (11)$$

$$\mathbf{D} = \epsilon \mathbf{E} \quad (12)$$

$$\rho = 0 \quad (13)$$

$$\mathbf{J} = \sigma \mathbf{E}, \quad (14)$$

Maxwell's equations become

$$\nabla \times \mathbf{E} = -i\omega \mathbf{B} \quad (15)$$

$$\nabla \times \mathbf{H} = (i\omega\epsilon + \sigma) \mathbf{E} \quad (16)$$

$$\nabla \cdot \mathbf{D} = 0 \quad (17)$$

$$\nabla \cdot \mathbf{B} = 0. \quad (18)$$

Using a vector identity we obtain

$$\nabla \times \nabla \times \mathbf{E} = \nabla(\nabla \cdot \mathbf{E}) - \nabla^2 \mathbf{E} \quad (19)$$

$$= -\nabla^2 \mathbf{E} \quad (20)$$

$$= -i\omega\mu\nabla \times \mathbf{H}, \quad (21)$$

from which the wave equation follows:

$$\nabla^2 \mathbf{E} = i\omega\mu(i\omega\epsilon + \sigma) \mathbf{E}. \quad (22)$$

Similarly, one may derive the wave equation for \mathbf{H}

$$\nabla^2 \mathbf{H} = i\omega\mu(i\omega\epsilon + \sigma) \mathbf{H}. \quad (23)$$

Region 1 (see Fig. 3) is free space, so that $\sigma = 0$, leading to

$$\nabla^2 \mathbf{E}_1 = -\omega^2 \mu_o \epsilon_o \mathbf{E}_1. \quad (24)$$

Picking the orientation of the electric field

$$\mathbf{E}_1 = \hat{x} E_1(x), \quad (25)$$

the solution to Eq.(24) is

$$\mathbf{E}_1 = \hat{x} \{ E_1^+ e^{-iky} + E_1^- e^{iky} \} \quad (26)$$

where

$$k^2 \equiv \omega^2 \mu_o \epsilon_o. \quad (27)$$

In region 2 we assume $\omega\epsilon \ll \sigma$ (i.e. the displacement current is negligible) yielding the wave equation

$$\nabla^2 \mathbf{E}_2 = i\omega\mu\sigma \mathbf{E}_2 \equiv \tau^2 \mathbf{E}_2 \quad (28)$$

where

$$\tau \equiv \frac{1+i}{\delta} = (1+i) \left(\frac{\omega\mu\sigma}{2} \right)^{1/2} \quad (29)$$

where δ is the skin depth of the conductor. The solution to Eq.(28) is then

$$\mathbf{E}_2 = \hat{x} \{ E_2^+ e^{-\tau y} + E_2^- e^{\tau y} \} \quad (30)$$

$$= \hat{x} E_2^+ e^{-\tau y} \quad (31)$$

since the electric field must be finite at $y \rightarrow \infty$. From Eq.(16) we have

$$\nabla \times \mathbf{H}_2 = \sigma \mathbf{E}_2 = \hat{x} \sigma E_2^+ e^{-\tau y} . \quad (32)$$

Therefore

$$\mathbf{H}_2 = \hat{y} H_y(z) + \hat{z} H_z(y) = \hat{z} H_2^+ e^{-\tau y} \quad (33)$$

where

$$H_2^+ = -\frac{\sigma}{\tau} E_2^+ \quad (34)$$

and $H_y(z) = 0$ since there is no z dependence. Applying the boundary equation that the tangential part of the electric field is continuous at the conductor surface yields

$$E_2^+ = E_1^+ + E_1^- \quad (35)$$

$$H_2^+ = -\frac{\delta\sigma(1-i)}{2} (E_1^+ + E_1^-) . \quad (36)$$

Again using Eq.(16), we have for the individual plane waves travelling to the right and to the left in region 1,

$$H_1^+ = -\left(\frac{\epsilon_o}{\mu_o}\right)^{1/2} E_1^+ \quad (37)$$

$$H_1^- = \left(\frac{\epsilon_o}{\mu_o}\right)^{1/2} E_1^- , \quad (38)$$

and therefore

$$\mathbf{H}_1 = \hat{z} (H_1^+ e^{-iky} + H_1^- e^{iky}) . \quad (39)$$

Applying this to the boundary condition that the tangential part of the magnetic intensity must be continuous yields

$$H_2^+ = H_1^+ + H_1^- = -\left(\frac{\epsilon_o}{\mu_o}\right)^{1/2} (E_1^+ - E_1^-) . \quad (40)$$

Using Eq.(36) and more algebra

$$E_2^+ = E_1^+ + E_1^- = \frac{4E_1^+}{2 + \sigma\delta Z_o(1-i)} \quad (41)$$

where $Z_o = (\mu_o/\epsilon_o)^{(1/2)}$ is the impedance of free space.

The time averaged power per unit area lost in the conductor (ρ_Ω) is given by the real part of the Poynting vector (\mathbf{N}) evaluated at $x = 0$;

$$\rho_\Omega = \Re \{ \langle \mathbf{N} \rangle |_{x=0} \} \quad (42)$$

where

$$\langle \mathbf{N} \rangle |_{x=0} = \frac{1}{2} \mathbf{E}_2 \times \mathbf{H}_2^* \quad (43)$$

$$= \hat{y} \frac{\sigma \delta}{4} (1+i) |E_2^+|^2 \quad (44)$$

$$= \hat{y} \frac{4(1+i) E_1^{+2}}{\sigma \delta [(Z_o + 2/\sigma \delta)^2 + Z_o^2]} \quad (45)$$

For reasonably good conductors and frequencies not too high, the factor

$$\frac{2}{\sigma \delta} = \left(\frac{2\omega \mu_o}{\sigma} \right)^{1/2} \quad (46)$$

is small compared to Z_o ($= 377\Omega$) and the heating density becomes

$$\rho_\Omega = \frac{(2E_1^+)^2}{2\sigma \delta Z_o^2} \quad (47)$$

In addition to being applicable to the case of a plane conductor, this equation is a good estimate of the heating density for a curved conductor when the radius of curvature is much larger than the wavelength of the radiation. Using Eq.(2) for a $\text{TEM}_{0,0,l}$ mode at the mirror we have

$$2E_1^+ = E_{o,l} \frac{w_{o,l}}{w_l(d/2)} \exp \left\{ -r^2 / w_l^2 (d/2) \right\} \quad (48)$$

Therefore, the power lost per mirror due to ohmic heating in a mirror of radius a at position d is

$$\begin{aligned} P_{\text{lost mirror}} &= \int_0^a \rho_\Omega 2\pi r \, dr \\ &= \frac{\pi E_{o,l}^2 w_{o,l}^2}{4\sigma \delta Z_o^2} \left[1 - \exp \left(\frac{-2a^2}{w_l^2 (d/2)} \right) \right] \end{aligned} \quad (49)$$

IV. Stored Energy

In vacuum, the time-averaged energy density is

$$u = \frac{1}{4} (\mathbf{E} \cdot \mathbf{D}^* + \mathbf{B} \cdot \mathbf{H}^*) = \frac{1}{2} \mathbf{E} \cdot \mathbf{D}^* \quad (50)$$

The total stored energy in the resonator is twice the stored energy due to the wave travelling in one direction given by Eq.(2). For a TEM_{0,0,l} mode this yields

$$\begin{aligned} E_{\text{stored}} &= \frac{\epsilon_o w_{o,l}^2 E_{o,l}^2}{4} \int_{-d/2}^{d/2} dy \int_0^a \frac{2\pi r dr}{w_l^2(y)} e^{-2r^2/w_l^2(y)} \\ &= \frac{\pi \epsilon_o E_{o,l}^2 w_{o,l}^2 d}{8} \left[1 - \exp\left(\frac{-2a^2}{w_l^2(d/2)}\right) \right] \end{aligned} \quad (51)$$

V. Ohmic Q

The ohmic Q of a cavity is defined as

$$Q_\Omega = \frac{\omega E_{\text{stored}}}{P_{\text{lost}}} \quad (52)$$

Noting that power is lost in two mirrors, and using Eqs.(49) and (51) we obtain

$$Q_\Omega = \frac{d}{2} (\pi f \mu_o \sigma)^{1/2} \quad (53)$$

where f is the frequency of the radiation.

VI. Resonator Heating

In this section we wish to calculate the time dependent rise in temperature of the resonator mirrors. To do so, we solve the one-dimensional heat equation with appropriate boundary conditions¹¹:

$$u_t(x, t) - \alpha u_{xx}(x, t) = \frac{A}{\rho c_v} \quad (54)$$

$$u(x, 0) = u_o \quad (55)$$

$$u_x(0, t) = 0 \quad (56)$$

$$u_x(L, t) = 0 \quad (57)$$

$$A = \mathcal{F} \delta(x) \quad (58)$$

where $u(x, t)$ is the temperature of the mirror at position x and time t , the subscripts of u denote partial derivatives of u , the mirror is located between $x = 0$ and $x = L$, \mathcal{F} is the flux incident on the mirror, and $\alpha = \kappa / (\rho c_p)$ where ρ , c_p , and κ are the mass density, heat capacity, and thermal conductivity of the mirror material.

The first step in solving this problem is to set $\mathcal{F} = A = 0$ and separate variables to find the eigenvalues and eigenvectors of the related homogeneous problem. Setting $u = X(x)T(t)$ and denoting derivatives by primes gives

$$\frac{T'}{\alpha T} = \frac{X''}{X} = -\lambda^2. \quad (59)$$

Therefore

$$X'' + \lambda^2 X = 0 \quad (60)$$

$$X'(0) = X'(L) = 0 \quad (61)$$

which has solutions

$$X_n(x) = \cos(\lambda_n x) \quad \lambda_n = \frac{n\pi}{L} \quad n = 0, 1, 2, \dots \quad (62)$$

Now let $A \neq 0$ and try the solution

$$u(x, t) = \sum_n T_n(t) X_n(x). \quad (63)$$

Multiplying by $u(x, t)$ and integrating yields

$$\begin{cases} T_0(t) &= \frac{1}{L} \int_0^L u(x, t) dx \\ T_m(t) &= \frac{2}{L} \int_0^L u(x, t) \cos\left(\frac{m\pi x}{L}\right) dx \quad m = 1, 2, \dots \end{cases} \quad (64)$$

Next we expand

$$A/(\rho c_p) = \sum_n q_n(t) X_n(x). \quad (65)$$

Inserting Eq.(58) gives

$$\begin{cases} q_0 &= \frac{\mathcal{F}}{\rho c_p L} \\ q_m &= \frac{2\mathcal{F}}{\rho c_p L} \quad m = 1, 2, \dots \end{cases} \quad (66)$$

Therefore the differential equation reduces to

$$\sum_n X_n (T'_n + \alpha \lambda_n^2 T_n - q_n) = 0 \quad (67)$$

Table 1: Parameters for the quasioptical IREC maser experiment.

Mode	TEM _{0,0,l}
Output power	15 MW
Frequency	280 GHz
Wavelength	1.1 mm
Magnetic field	6 T
Electron beam energy	500 keV
Electron beam current	200 A
F	0.2
$\alpha \equiv \beta_{\perp}/\beta_{\parallel}$	0.5
ψ	20°
μ	12

which leads to

$$\begin{cases} u_0 + q_0 t & n = 0 \\ -\frac{q_n}{\lambda_n^2 \alpha} [\exp(-\lambda_n^2 \alpha t) - 1] & n = 1, 2, \dots \end{cases} \quad (68)$$

Thus the solution for the mirror temperature is

$$u(x, t) = u_0 + \frac{\mathcal{F}t}{\rho c_p L} + \frac{2\mathcal{F}L}{\pi^2 \kappa} \sum_{n=1}^{\infty} \frac{1}{n^2} \cos\left(\frac{n\pi x}{L}\right) \left[1 - \exp\left(\frac{-n^2 \pi^2 \alpha t}{L^2}\right)\right]. \quad (69)$$

VII. The IREC Maser Resonator

In this section the formulae derived will be applied to the current design of the resonator for the quasioptical IREC maser experiment. Representative experimental parameters are given in Table 1. The theory necessary to optimize an IREC maser design is complicated and will be addressed in future publications, however, let us pick $F = 0.2$ for this example. This value is approximately twice the F value for optimum efficiency operation in a QOG and is appropriate for the IREC maser since here the beam electrons interact only with

the RF fields propagating in the direction of the electron beam travel. Also picked are values for the angle between the resonator and electron axes $\psi = 20^\circ$ and the normalized interaction length $\mu = 12$. Specifying the peak heating density at the mirror to be 150 kW/cm^2 determines the resonator mirror separation (81 cm) and radius of curvature (52 cm). The output coupling of 14% is picked to balance the input and output power levels and determines the mirror radius of 3.0 cm. Assuming values for the conductivity ($3.6 \times 10^7 \text{ siemens/m}$) and the skin depth ($1.6 \times 10^{-7} \text{ m}$), appropriate for copper, Eq.(49) may be used to calculate the power lost per mirror (780 kW).

With the resonator parameters specified, it is a simple matter to apply the derived formulae to obtain the peak electric field at the center of the resonator (Eq.(9)) $E_o = 1.1 \text{ MV/cm}$. Similarly, the energy stored in the resonator (Eq.(51)) is $E_{\text{stored}} = 2.4 \text{ J}$, and the ohmic quality factor (Eq.(53)) is $Q_\Omega = 2.5 \times 10^6$. The resonator heating is calculated assuming that the incident flux is $\mathcal{F} = 150 \text{ kW/cm}^2$, the peak heating density. Eq.(69) then gives a temperature rise at the surface of the mirror of approximately 150°C for a $2 \mu\text{sec}$ pulse. Standard values for copper of $\rho = 8.93 \text{ g/cm}^3$, $c_p = 0.385 \text{ J/(g}^\circ\text{K)}$, $\kappa = 3.5 \text{ W/cm}^\circ\text{K}$, $\alpha = 1.02 \text{ cm}^2/\text{sec}$, and a mirror thickness of $L = 1 \text{ cm}$ were used in this calculation. It should be noted that the number of terms necessary for the convergence of the sum in Eq.(69) is approximately 1000. Figure 4 shows that at the end of $2 \mu\text{sec}$ the temperature rise in the mirror is confined to very near its surface. The parameters calculated for the IREC maser resonator are summarized in Table 2.

VIII. Acknowledgements

We thank Drs. Arne Fliflet and Wallace Manheimer for their helpful discussions. This work was supported by the Office of Fusion Energy of the U.S. Department of Energy and by the Office of Naval Research.

Table 2: Calculated parameters for the quasioptical IREC maser experiment.

Mirror separation (d)	81 cm
Mirror radius of curvature	52 cm
Output coupling	14 %
Mirror radius	3.0 cm
E_o	1.1 MV/cm
w_o	8.5 mm
$w(d/2)$	1.8 cm
z_o	21 cm
Quality factor (diffraction, Q_{diff})	66,000
Quality factor (ohmic, Q_{Ω})	2.5×10^6
$\rho_{\Omega_{\text{peak}}}$	150 kW/cm ²
Ohmic power lost (per mirror)	780 kW

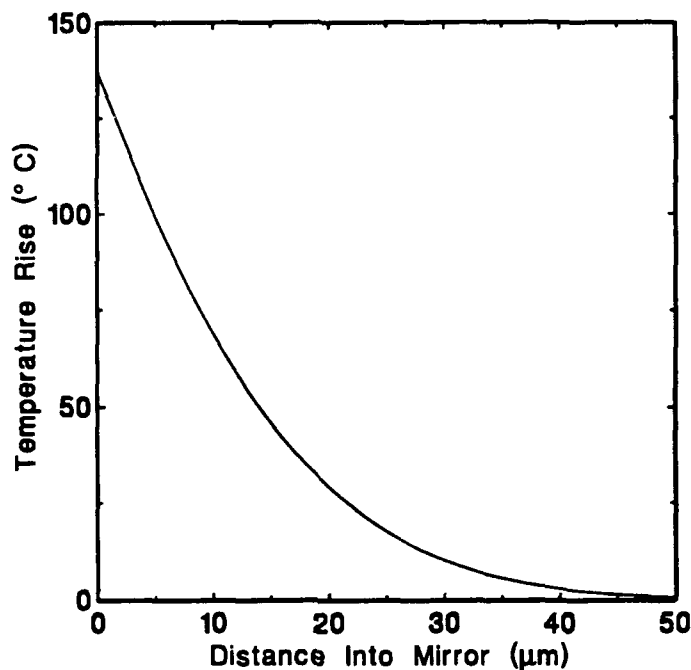


Figure 4: Temperature rise in the resonator mirror calculated from a one-dimensional model for an incident power flux (\mathcal{F}) of 150 kW/cm^2 and a $2 \mu\text{sec}$ pulse length.

References

- ¹ P. Sprangle, J. Vomvoridis and W. M. Manheimer, Appl. Phys. Lett. **38**, 310 (1981), and Phys. Rev. A **23**, 3127 (1981).
- ² T. A. Hargreaves, K. J. Kim, J. H. McAdoo, S. Y. Park, R. D. Seeley, and M. E. Read, Int. J. Elec. **57**, 977 (1984).
- ³ A. W. Fliflet, T. A. Hargreaves, W. M. Manheimer, R. P. Fischer, and M. L. Barsanti, Phys. Rev. Lett. **62**, 2664 (1989).
- ⁴ A. W. Fliflet, T. A. Hargreaves, W. M. Manheimer, R. P. Fischer, M. L. Barsanti, B. Levush, and T. Antonsen, Phys. Fluids B **2**, 1046 (1990).
- ⁵ T. Antonsen, B. Levush, and W. M. Manheimer, Phys. Fluids B, **2**, 419 (1990).
- ⁶ A. W. Fliflet, to be published.

- ⁷ A. Yariv, *Optical Electronics* (CBS College Publishing, New York, NY, 1985).
- ⁸ B. G. Danly and R. J. Temkin, *Phys. Fluids* **29**, 561 (1986).
- ⁹ T. M. Tran, B. G. Danly, K. E. Kreischer, J. B. Schutkeker, and R. J. Temkin, *Phys. Fluids* **29**, 1274 (1986).
- ¹⁰ S. Ramo, J. R. Whinnery, and T. Van Duzer, *Fields and Waves in Communication Electronics* (John Wiley & Sons, Inc., New York-London-Sydney, 1965).
- ¹¹ R. L. Street, *Partial Differential Equations* (Wadsworth Publishing Company, Inc., Belmont, California 94002, 1973).

4793/4 DISTRIBUTION LIST

Air Force Avionics Laboratory AFWAL/AADM-1 Wright/Patterson AFB, OH 45433 Attn: Walter Friez	1 copy
Air Force Office of Scientific Research Bolling AFB Washington, DC 20332 Attn: H. Schlossberg	1 copy
Air Force Weapons Laboratory Kirtland AFB Albuquerque, NM 87117 Attn: Dr. W. Baker Dr. A.H. Guenter	2 copies 1 copy
Columbia University 520 West 120th Street Department of Electrical Engineering New York, NY 10027 Attn: Dr. S.P. Schlesinger Dr. A. Sen	1 copy 1 copy
Columbia University 520 West 120th Street Department of Applied Physics and Nuclear Engineering New York, NY 10027 Attn: Dr. T.C. Marshall Dr. R. Gross	1 copy 1 copy
Cornell University School of Applied and Engineering Physics Ithaca, NY 14853 Attn: Dr. H. Fleischmann Dr. J. Nation Dr. R.N. Sudan	1 copy 1 copy 1 copy
Creol-FEL Research Pavillion 12424 Research Parkway, Suite 400 Orlando, FL 32826 Attn: Dr. L.R. Elias Dr. I. Kimel	1 copy 1 copy

Dartmouth College 18 Wilder, Box 6127 Hanover, NH 03755 Attn: Dr. J.E. Walsh	1 copy
Defense Advanced Research Project Agency, DEO 1400 Wilson Blvd. Arlington, VA 22209 Attn: Dr. L. Buchanan	1 copy
Defense Communications Agency Washington, DC 20305 Attn: Dr. P.C. Jain, Assistant for Communications Technology	1 copy
Defense Nuclear Agency Washington, DC 20305 Attn: Dr. L. Wittwer (RAAE)	5 copies
Defense Technical Information Center Cameron Station 5010 Duke Street Alexandria, VA 22314	2 copies
Department of Energy Division of Advanced Energy Projects Washington, DC 20545 Attn: Dr. R. Gajewski	1 copy
Department of Energy Office of Energy Research Washington, DC 20545 Attn: C. Finfgeld/ER-542, GTN T.V. George/ER-531, GTN D. Crandall/ER-54, GTN Dr. David F. Sutter/ER-224, GTN	1 copy 1 copy 1 copy 1 copy
Director of Research U.S. Naval Academy Annapolis, MD 21402-5021	2 X copy
General Atomics 13-260 Box 85608 San Diego, CA 92138 Attn: Dr. J. Doane Dr. C. Moeller	1 copy 1 copy

Georgia Institute of Technology, EES-EOD Baker Building Atlanta, GA 30332 Attn: Dr. James J. Gallagher	1 copy
Hanscomb Air Force Base Stop 21, MA 01731 Attn: Lt. Rich Nielson/ESD/INK	1 copy
Hughes Aircraft Co. Electron Dynamics Division 3100 West Lomita Boulevard Torrance, CA 90509 Attn: J. Christiansen J. Tancredi	1 copy 1 copy
Hughes Research Laboratory 3011 Malibu Canyon Road Malibu, CA 90265 Attn: Dr. R. Harvey Dr. R.W. Schumacher	1 copy 1 copy
KMS Fusion, Inc. 3941 Research Park Dr. P.O. Box 1567 Ann Arbor, MI 48106 Attn: S.B. Segall	1 copy
Lawrence Berkeley Laboratory University of California 1 Cyclotron Road Berkeley, CA 94720 Attn: Dr. A.M. Sessler	1 copy
Lawrence Livermore National Laboratory P.O. Box 808 Livermore, CA 94550 Attn: Dr. D. Prosnitz Dr. T.J. Orzechowski Dr. J. Chase Dr. W.A. Barletta Dr. D.L. Birk Dr. E.T. Scharlemann	1 copy 1 copy 1 copy 1 copy 1 copy 1 copy
Litton Electron Devices 960 Industrial Road San Carlos, CA 94070 Attn: Library	1 copy

Los Alamos National Laboratory
P.O. Box 1663, MSJ 564
Los Alamos, NM 87545
Attn: Dr. B. Newnam 1 copy

Los Alamos National Laboratory
P.O. Box 1663, AT5-827
Los Alamos, NM 87545
Attn: Dr. T.J.T. Kwan 1 copy
Dr. L. Thode 1 copy
Dr. R.R. Bartsch 1 copy

Massachusetts Institute of Technology
Department of Physics
Cambridge, MA 02139
Attn: Dr. G. Bekefi/36-213 1 copy
Dr. M. Porkolab/NW 36-213 1 copy
Dr. R. Davidson/NW 16-206 1 copy
Dr. A. Bers/NW 38-260 1 copy
Dr. K. Kreischer 1 copy
Dr. B. Danly 1 copy
Dr. G.L. Johnston 1 copy

Massachusetts Institute of Technology
167 Albany St., N.W. 16-200
Cambridge, MA 02139
Attn: Dr. R. Temkin/NW 14-4107 1 copy

Mission Research Corporation
8560 Cinderbed Road, Suite 700
Newington, VA 22122
Attn: Dr. M. Bollen 1 copy
Dr. J. Pasour 1 copy

Naval Research Laboratory
Addressee: Attn: Name/Code
Code 0124 - ONR 1 copy
Code 1000 - Commanding Officer 1 copy
Code 1001 - T. Coifey 1 copy
Code 1003.9A - Computer Resources Architect 1 copy
Code 1005 - Head, Office of Mgt. and Admin. 1 copy
Code 1005.1 - Deputy Head, Off. of Mgt. and Admin. 1 copy
Code 1005.6 - Head, Directives Staff 1 copy
Code 1200 - Capt. R.W. Michaux 1 copy
Code 1201 - Deputy Head, Command Support Division 1 copy
Code 1220 - Security 1 copy
Code 2000 - J. Brown 1 copy

Code 3000 - R. Doak	1 copy
Code 4000 - R. Ellis	1 copy
Code 4600 - D. Nagel	1 copy
Code 4700 - S. Ossakow	26 copy
Code 4700.1 - A. Ali	1 copy
Code 4707 - W. Manheimer	1 copy
Code 4770 - G. Cooperstein	1 copy
Code 4790 - Branch Office	5 copy
Code 4790 - W.M. Black	1 copy
Code 4790 - A.W. Fliflet	1 copy
Code 4790 - S.H. Gold	1 copy
Code 4790 - T. Hargreaves	1 copy
Code 4790 - C. Hui	1 copy
Code 4790 - C. Kapetanacos	1 copy
Code 4790 - A.K. Kinhead	1 copy
Code 4790 - Y.Y. Lau	1 copy
Code 4790 - M. Rhinewine	1 copy
Code 4790 - P. Sprangle	1 copy
Code 5700 - L. Cosby	1 copy
Code 6840 - S. Ahn	1 copy
Code 6840 - C. Armstrong	1 copy
Code 6840 - A. Ganguly	1 copy
Code 6840 - R. Parker	1 copy
Code 6840 - N. Vanderplaats	1 copy
Code 6850 - L. Whicker	1 copy
Code 6875 - R. Wagner	1 copy

Naval Sea Systems Command
 Department of the Navy
 Washington, DC 20362
 Attn: Commander, PMS 405-300

1 copy

Northrop Corporation
 Defense Systems Division
 600 Hicks Rd.
 Rolling Meadows, IL 60008
 Attn: Dr. Gunter Dohler

1 copy

Oak Ridge National Laboratory
 P.O. Box Y
 Mail Stop 3
 Building 9201-2
 Oak Ridge, TN 37830
 Attn: Dr. A. England

1 copy

Office of Naval Research 800 N. Quincy Street Arlington, VA 232217 Attn: Dr. C. Roberson	1 copy
Office of Naval Research 1012 W. 36th Street, Childs Way Bldg. Los Angeles, CA 90089-1022 Attn: Dr. R. Behringer	1 copy
Optical Sciences Center University of Arizona Tucson, AZ 85721 Attn: Dr. Willis E. Lamb, Jr.	1 copy
Physical Sciences Inc. 603 King Street Alexandria, VA 22314 Attn: M. Read	1 copy
Physics International 2700 Merced Street San Leandro, CA 94577 Attn: Dr. J. Benford	1 copy
Princeton Plasma Physics Laboratory James Forrestal Campus P.O. Box 451 Princeton, NJ 08544 Attn: Dr. H. Hsuan Dr. D. Ignat Dr. H. Furth Dr. P. Efthimion Dr. F. Perkins	1 copy 1 copy 1 copy 1 copy 1 copy
Raytheon Company Microwave Power Tube Division Foundary Avenue Waltham, MA 02154 Attn: N. Dionne	1 copy
Sandia National Laboratory Org. 1231, P.O. Box 5800 Albuquerque, NM 87185 Attn: Dr. Thomas P. Wright Mr. J.E. Powell Dr. J. Hoffman Dr. W.P. Ballard Dr. C. Clark	1 copy 1 copy 1 copy 1 copy 1 copy

Science Applications International Corp.

1710 Goodridge Dr.

McLean, VA 22102

Attn: Dr. A. Drobot

1 copy

Dr. P. Vitello

1 copy

Dr. D. Bacon

1 copy

Dr. C. Menyuk

1 copy

Science Research Laboratory

15 Ward Street

Somerville, MA 02143

Attn: Dr. R. Shefer

1 copy

SPAWAR

Washington, D.C. 20363

Attn: E. Warden, Code PDE 106-3113

1 copy

Capt. Fontana

1 copy

Spectra Technologies

2755 Northup Way

Bellevue, WA 98004

Attn: Dr. J.M. Slater

1 copy

Stanford University

Department of Electrical Engineering

Stanford, CA 94305

Attn: Dr. J. Feinstein

1 copy

Stanford University

High Energy Physics Laboratory

Stanford, CA 94305

Attn: Dr. T.I. Smith

1 copy

Stanford University

SLAC

Stanford, CA 94305

Attn: Dr. Jean Labacqz

1 copy

TRW, Inc.

One Space Park

Redondo Beach, CA 90278

Attn: Dr. H. Boehmer

1 copy

Dr. T. Romisser

1 copy

Dr. Z. Guiragossian

1 copy

University of California
Physics Department
Irvine, CA 92717
Attn: Dr. G. Benford
Dr. N. Rostoker

1 copy
1 copy

University of California
Department of Physics
Los Angeles, CA 90024
Attn: Dr. A.T. Lin
Dr. N. Luhmann
Dr. D. McDermott

1 copy
1 copy
1 copy

University of Maryland
Department of Electrical Engineering
College Park, MD 20742
Attn: Dr. V.L. Granatstein
Dr. W.W. Destier

1 copy
1 copy

University of Maryland
Laboratory for Plasma and Fusion Energy Studies
College Park, MD 20742
Attn: Dr. Tom Antonsen
Dr. John Finn
Dr. Jhan Varyan Hellman
Dr. W. Lawson
Dr. Baruch Levush
Dr. Edward Ott
Dr. M. Reiser

1 copy
1 copy
1 copy
1 copy
1 copy
1 copy
1 copy

University of New Mexico
Department of Physics and Astronomy
800 Yale Blvd., N.E.
Albuquerque, NM 87131
Attn: Dr. Gerald T. Moore

1 copy

University of Tennessee
Department of Electrical Engineering
Knoxville, TN 37916
Attn: Dr. I. Alexeff

1 copy

University of Utah
Department of Electrical Engineering
3053 Merrill Engineering Bldg.
Salt Lake City, UT 84112
Attn: Dr. Larry Barnett
Dr. J. Mark Baird

1 copy
1 copy

U.S. Army
Harry Diamond Laboratories
2800 Powder Mill Road
Adelphi, MD 20783-1145

Attn: Dr. H. Brandt	1 copy
Dr. E. Brown	1 copy
Dr. S. Graybill	1 copy
Dr. A. Kehs	1 copy
Dr. J. Silverstein	1 copy

Varian Associates
611 Hansen Way
Palo Alto, CA 94303

Attn: Dr. H. Huey	1 copy
Dr. H. Jory	1 copy
Dr. K. Felch	1 copy
Dr. R. Pendleton	1 copy
Dr. A. Salop	1 copy

Varian Eimac San Carlos Division
301 Industrial Way
San Carlos, CA 94070
Attn: Dr. C. Marshall Loring

1 copy

WL/CA
Kirtland AFB, NM 87117-6008
Attn: Dr. Brendan B. Godfrey

1 copy

Yale University
Department of Applied Physics
Madison Laboratory
P.O. Box 2159
Yale Station
New Haven, CT 06520
Attn: Dr. I. Bernstein

1 copy

Do Not make labels for
Records----- (1 cy)
Code 4828---- (22 cys)

Naval Research Laboratory
Washington, DC 20375-5000
Code 4830
Timothy Calderwood